Gait Parameters Estimation from Sensor-Belt IMU Data

Roland Stenger, Hawzhin Hozhabr Pour, Jonas Teich, Andreas Hein, and Sebastian Fudickar,

***Abstract* — Changes in gait are associated with an increased risk of falling and may indicate the presence of movement disorders in connection with a neurological disease or age-related weakness. Continuous monitoring, based on inertial measurement unit (IMU) sensor data can be used to estimate gait parameters that indicate changes in gait. The monitoring from a waist-level IMU sensor is applicable for the assessment of such data, as it can be easily worn either as specific sensor-integrated belts or being suitable as a smartphone application. However, there is also the challenge that data from a waist-level mounted sensor provides a weaker representation of gait compared to signals from sensors placed closer to the legs and feet as sources of motion. Our work examines how well gait parameters can be estimated from the data of a waist worn IMU sensor. The approach employs the processing of the IMUs triaxial accelerometer and gyroscope data to detect gait events and estimate spatio-temporal gait parameters. In addition to the gait events heel strike (HS) and toe off (TO), it estimates the gait parameters step length, cadence, speed, stance time, swing time, and stride time. The results are compared to data measured by a GAITRite® system as a reference. The present study investigates and compares the accuracy of two different approaches for gait event detection: a rule-based method and a machine learning (ML) approach based on a sequence-to-sequence convolutional neural network (CNN) architecture. The efficacy of these approaches in accurately determining gait parameters is evaluated using a dataset consisting of 21,193 recorded steps from 70 subjects, who performed 4,590 walks, each with a distance of approximately 4 meters. The ML-based algorithm performs better than the rule-based achieving an accuracy of over 99% in detecting gait events and estimating step lengths with a mean error of -0.12±4.49 cm.**

***Index Terms*— Biomedical computing, Biomedical signal processing, Inertial sensors, Wearable sensors, Motion estimation, Gait recognition, Time series analysis, Deep learning, Learning systems, Convolutional neural networks, Machine learning**

Roland Stenger is with the Institute for Medical Informatics, University of Lübeck, 23562 Germany (e-mail: roland.stenger@uni-luebeck.de).

Hawzhin Hozhabr Pour is with the Institute for Medical Informatics, University of Lübeck, 23562 Germany (e-mail: hawzhin.hozhabrpour@uni-luebeck.de).

Jonas Teich is with the Carl von Ossietzky University Oldenburg, 26111 Germany (e-mail: jonas.teich@uni-oldenburg.de).

Andreas Hein is with the Group Assistance Systems and Medical Device Technology, Department of Health Services Research, Carl von Ossietzky University Oldenburg, 26111 Germany (e-mail: andreas.hein@uol.de).

Sebastian Fudickar is with the Institute for Medical Informatics, University of Lübeck, 23562 Germany (e-mail: sebastian.fudickar@uni-luebeck.de).

Digital Object Identifier

I. Introduction

Gait analysis enables the identification of age-related muscular-skeletal diseases and (neurological) movement disorders and supports the quantification of disease-progression. For instance, gait patterns characterized by shuffled, small steps, or lower gait velocities are associated with increased fall risks [1]. A previous study showed a correlation (confidence coefficient ranging from 0.595 to 0.798) between gait velocity, step/stride length and the Berg Balance Scale [2]. It has also been shown that gait consistency and variability differ in people, who fell within a 3-day study phase, compared with the healthy control [3]. Changes in the gait pattern can also be seen at an early stage of Parkinson's disease [4], [5]. Another study showed that gait velocity is associated with survival in the elderly population [6]. It is therefore important to recognize such patterns as early as possible. However, regular in-person screenings by specialists are considered unpractical, due to limited health-care resources, patient-discomfort and lack of acceptance resulting from long travel distances, time-requirements, and/or belief in their own healthiness [7].

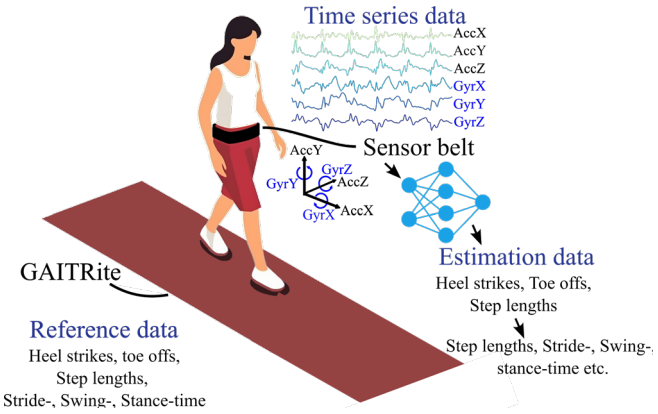

Fig. 1. Schematic overview of the data that is used is this work. The reference data comes from GAITRite®, while the algorithms make estimations based on the measurements of the IMU sensor.

Gait analysis systems such as floor-based gait tracking [8], [9] or camera-based systems with 3D or RGB cameras, with or without markers [10]–[13], can be used to estimate spatio-temporal gait parameters (e.g., step length, velocity, swing/stance time etc.). However, such systems are only applicable for specific research settings, as such systems require specialized users, complex room setups (sensor carpet

implementation, advanced camera setup) or extended subject-preparation times (e.g., for setting up markers on subjects). Continuous screening via camera based systems in everyday life is also impracticable due to privacy concerns that arise in private environments. Furthermore, the installation of sensor carpets or camera based systems in the home environment incurs considerable installation costs and typically restricts the coverage of the monitoring capabilities to certain living areas. Therefore, such ambient sensors are unsuitable for continuous gait analysis in everyday living.

Inertial measurement unit-based systems (IMU) represent a cost-effective option for gait analysis in everyday life. IMUs include gyroscope and accelerometer and are nowadays integrated in most mobile-phones, thus available in "everyone's pocket's". IMUs are predominantly used at the subject's ankle or calf for the estimation of spatio-temporal gait parameters, as they have a well-documented history of effectiveness in this application [14]. The placement on the ankle or calf is a common variant, but it is another necessary device that must be placed on the body. One advantage here would be the use of smartphone sensors. The data from our waist-worn sensor (between the L3 and the L5 lumbar vertebral [15]) is in this regard more similar to the data that smartphones would record. Previous studies explore the IMU data processing from a sensor placed at hip level, on diseased subjects with mobility affected conditions, such as PD and Multiple Sclerosis (MS) [16] [17]. They also discuss the advantages of a waist or hip worn sensor. Previous studies have explored the processing of IMU data from a sensor placed at the hip level on subjects with mobility-affected conditions, such as PD and Multiple Sclerosis (MS) [16] [17]. These studies have discussed the advantages of their sensor placement being unobtrusively and comfortably to wear.

To address the challenge of IMU-based gait analysis, we investigate two algorithmic approaches for the spatio-temporal gait parameters based on the waist-worn (L2) IMU sensor compared to a GAITRite® reference sensor-system, as visualized in Fig. 1. The GAITRite® is a validated tool for gait parameter estimation [18]. We propose and evaluate a two-stage algorithm. The first stage of the algorithm is the detection of HS and TO events, which is performed through either a rule-based approach or an ML-based approach for comparison. The second stage, step length estimation, is exclusively ML-based. Three variations were evaluated: (1) rule-based HS/TO detection with ML-based step length estimation (without subject meta-information), (2) ML-based HS/TO detection with ML-based step length estimation (without meta-information), and (3) ML-based HS/TO detection with ML-based step length estimation (with meta-information). The algorithm employs the detection of HS/TO events and the estimation of step lengths to compute a range of gait parameters, including cadence, velocity, step time, swing time, and stance time. Additionally, we discuss existing method performances, in comparison to these proposed approaches, and point out the need for a common/standardized evaluation scheme to enable comparison among results.

II. Related Work

The processing of IMU sensor data for gait analysis is a research area with a great variety of approaches. In the following, the core directions and trends in this context are identified, focusing on the use case, sensor position/number, type of gait parameters, and type of algorithmic data processing. When discussing gait analysis in the following, we refer to the algorithmic processing of IMU-based data with the objective of extracting features of the gait, such as the timing of the HS, stride length, and so forth.

A. Use Cases

The necessity for gait metrics analysis is motivated by a variety of use cases. The review of gait-metrics analysis with IMU sensors [19] evaluates the type of cohort groups for the studies considered and concludes that the majority of studies include healthy subjects, followed by older subjects (to cover age-related movement disorders), Parkinson's disease (PD), post-stroke with ataxia (stroke-related impairment), Huntington's disease, and lower limb amputees. The authors did not explicitly use any of these impairments as keywords in their literature search. The review paper [14] also lists the use cases of the studies included in the paper, whereby multiple mentions are possible insofar as studies considered multiple impairments within the same study. Stroke-related impairments are most frequently represented here (11 out of 30 mentions). The next most frequently mentioned impairments are amputations and cerebral palsy, with four mentions each, followed by PD with three. The authors did not explicitly use any of these impairments as keywords in the literature search as well.

B. Sensor Positions

This section provides a summary of the positioning of IMU sensors and their combinations in past studies, with the objective of identifying the most common constellations. In a review, presented in [14], a total of 113 studies, related to gait analysis, were evaluated. Their findings indicate that up to the year 2020, IMU sensors were most frequently placed on the shank (with 39 of 114 studies) and foot (with 38 studies). The frequency of utilization of sensors at the tight and trunk, follow. However, these placements—at the tight and trunk—are rarely observed as single sensor settings. In fact, approximately 33% of tight placements and 25% of trunk placements include only one sensor. Instead, they are often incorporated into a combined placement. It was observed that the combination of shank and tight placements was most frequently used. In another study [20], although no meaningful comparison can be made with regard to usability, as they argue, due to the heterogeneity of the studies, they list the sensor placement of 38 evaluated studies. The placement is significantly different here. The wrist is the most frequently studied placement, with 16 studies, followed by the waist and hip, with nine and eight studies, respectively. Chest placement is represented in 7 studies (comparable to trunk). In another review paper [19], studies with single sensor settings were

evaluated. The results indicated that the waist was chosen by a large majority (30 of 42 studies). It is important to note that the studies were designed for distinct purposes, which implies that the selection of sensor positions is contingent upon the specific context.

C. Algorithms

According to Cicirelli et al. [21], support vector machines have been the most used method for neurodegenerative diseases such as Alzheimer's disease, PD, MS or Amyotrophic Lateral Sclerosis (ALS) up to the beginning of 2021. However, recent advances in the field of deep learning have led to the development of methods such as convolutional neural networks (CNNs) and long-short-term-memories (LSTMs). While the effectiveness of these methods is dependent on the availability of large amounts of data, instance-based and tree-based methods have shown promising results with limited data. The systematic review [14] covers various algorithms and highlights rule-based methods using threshold or peak detection as the most widely used for gait detection (such as HS or TO). The authors argue that rule based algorithms are particularly effective for real time applications, for example in clinical settings where timely and accurate gait analysis is essential, due to the algorithms' low computational complexity. Such rule-based methods are covered by 63 out of 92 studies. It should be noted that in this case the use case is based on gait event detection and no spatial or spatio-temporal parameters are estimated. In the same evaluation, ML algorithms play a role in 19 of the 92 studies.

TABLE I
SENSOR POSITIONS, NUMBER OF SENSORS EMPLOYED AND TYPE OF ALGORITHMIC APPROACH IN PREVIOUS WORK. THE BEST PERFORMING ALGORITHM IN THIS PAPER IS LABELED AS *ML-Seq2Seq*. RNN=RECURRENT NEURAL NETWORK

Source	Algorithm	Type	Sensor position(s)	N Sensors
[22]		RB	Waist, Shanks	3
[23]		RB	Right foot	1
[24]		RB	Shanks	2
[25]		RB	Shanks, Feet	5
[26]	CNN	ML	Ankle joints, Shanks	4
[27]	CNN	ML	Chest, Lower back, Right Hand, Wrist, Right knee, Right ankle	5
[28]	CNN, RNN	ML	Right foot	1
[29]	CNN, RNN	ML	Waist	1
[30]	Decision tree	ML	Right foot	1
[31]	CNN	ML	Pelvis, Thigh, Shank, Feet	7
[32]	CNN	ML	Ankle joints	2
[33]	CNN	ML	Shanks	2
ML-Seq2Seq	CNN	ML	Waist	1

For a meaningful comparison with our work, Fig. 2 shows articles that employ IMU sensors to record the gait of only healthy adults walking in a straight line. A qualitative comparison can be found in Section V. The graphic presented here serves as an overview of which gait parameters are included in the respective papers' evaluation. Without claiming to be comprehensive, in the previous work introduced here, no rule-based algorithm estimates any spatial or spatio-temporal gait parameter. The estimation of HS and TO events is a predominant focus. Storm et al. [22] is the only study that derives temporal parameters, including step, stride, and stance times, from the events. In the ML-based algorithms, these papers in which only gait events are estimated also predominate. However, in three of these papers, a number of other parameters are determined. The reasons for the disparate compositions may be manifold. In order to implement an algorithmic estimation, a dataset with the requisite labels must be available. It appears that rule-based methods are not well-suited for estimating spatial or spatio-temporal parameters.

A comparison of the proposed algorithms with regard to sensor positioning, as additionally shown in Table I, reveals that almost all papers (11/13) utilize sensors that are worn on the lower body. The most common position for the sensors is at the shank. The foot as sensor placement is notable frequently used (5/13). In contrast, positions such as the waist, ankle, chest, knee, pelvis, and thigh have fewer sensors (up to 2/13).

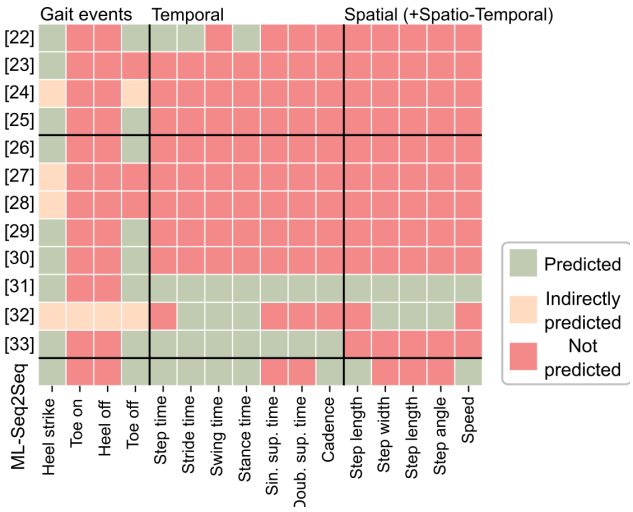

Fig. 2. Gait parameters estimated in the respective studies. A yellow marker indicates that the respective gait parameter was estimated in a broader sense. This means that instead of estimating the parameter directly, estimations were made based on another related parameter. For example, estimations could involve the time span of the load response phase, measured from the moment of the HS to the next TO marking the beginning and end of such phase. If in this example, only the load response is considered in the evaluation, we still interpret this as indirect evaluation of the HS and TO timings and mark it as yellow. The best performing algorithm in this paper is labeled as *ML-Seq2Seq*.

III. MATERIALS AND METHODS

This section outlines the methodology used in the study, starting with a description of the dataset which was collected using an IMU sensor and the GAITRite® system. The pre-processing steps on the dataset are then detailed, involving synchronization and data cleaning. Two gait event detection algorithms are explained: a rule-based method and an ML-based model. The methodology also includes step length estimation and the calculation of additional gait parameters, which in combination with the gait event detection approach

form a two-stage algorithm. Finally, the evaluation methods and performance metrics for the algorithms are presented.

A. Data Description

The study dataset was collected at the University of Oldenburg, employing a single IMU sensor integrated into a waist-worn Humotion sensor belt between the L3 and the L5 lumbar vertebral [2]. Informed consent was given for the use of data for scientific purposes. The IMU sensor features a triaxial accelerometer, gyroscope, and magnetometer, each sampled at 100 Hz. The placement and orientation of the sensor were adjusted according to the hip circumference of each participant to ensure stability and uniformity, crucial for accurate gait recording. Fig. 3 shows the sensor data of a single walk with the gait events HS and TO during a 4-meter walk.

The GAITRite® system, a validated tool for gait parameter estimation [18], was used as reference, recording gait alongside the sensor belt. It records event-based measurements, capturing the exact time and location of foot contacts on its sensor grid, which are spaced at a minimum of 1.27 cm apart [9].

As summarized in Table II, the study involved 86 subjects ranging from 21 to 82 years of age, each performing several walks in two velocities (slow and fast) over a distance of 4 meters. A total of 7877 walks and 56351 steps were recorded over approximately eight hours.

TABLE II
STATISTICS OF THE STUDY COHORT AND THE CONSIDERED DATA.

	Parameter	Mean (Std)	Min/Max
Subjects	N=70		
	Height [cm]	173 (10)	151/196
	Weight [kg]	77 (13)	53/103
	Age [years]	60 (23)	21/82
	Walks per subject	66 (16)	28/92
Walks	N=4590		
	Walk duration [ms]	3210 (725)	2000/710
	Steps per walk	4.6 (1.2)	2/12
Steps	N=21193		
	Step length [cm]	60.98 (8.68)	29.04/96.46
	Stride time [ms]	568 (61)	380/1680
	Stance time [ms]	154 (37)	20/850
	Swing time [ms]	419 (38)	290/767
	Cadence [s^{-1}]	106.2 (10.8)	81.0/186.0
	Speed [m/s]	1.11 (0.18)	0.63/1.76

B. Preprocessing

The following preprocessing steps were applied:

Step length extraction: The step length is calculated from the raw GAITRite® data as the spatial Euclidean distance d between the (x, y)-positions of two consecutive HS of the same foot as

$$d = \sqrt{(x_{\mathrm{HS2}} - x_{\mathrm{HS1}})^2 + (y_{\mathrm{HS2}} - y_{\mathrm{HS1}})^2}.$$

Synchronization: The time series $x(t)$ from the IMU with the GAITRite® data are synchronized by aligning the timestamps of the IMU data t_{IMU} with the absolute timestamps of the GAITRite® t_{G} data as

$$\Delta t = \| t_{\mathrm{IMU}} - t_{\mathrm{G}} \|,$$
$$\tilde{x}(t) = x(t - \Delta t).$$

Data cleaning: Data cleaning was necessary to ensure the integrity of the dataset. Some recorded walks lacked sensor belt data or GAITRite® data, which were subsequently excluded from further consideration. Of the 86 datasets, 70 were retained for use in this study. Walks with a duration below 2 seconds (200 time steps) are not considered in developing the algorithm that outputs temporal intervals with a minimum length of 2 seconds. Additionally, any walk during which the GAITRite® system failed to detect at least one step was also removed. Steps not detected are identified when the duration of the previous one is significantly longer than usual, specifically more than 150% of the median step time of that walk. This resulted in 36 walks being discarded, about 0.8% of all data. Moreover, walks where a single step was recorded by mistake as two separate steps were eliminated. These 'double steps' are identified when the step time is less than 10% of the median step time. This further reduced the dataset by 32 walks, which represents approximately 0.7% of the initial data pool. From each pair of double steps, the first one was discarded.

Trimming Walk Data: The data is trimmed by removing all time steps before the first HS and after the last HS of each walk on the basis of the GAITRite® data, to filter time periods where no step length can be extracted, as one step is defined as the interval between two HS.

Final preprocessing: Finally, a step length is assigned to each time step in the IMU time series, using the GAITRite® reference data, which provide a corresponding step length for all time steps in between each pair of consecutive HS. All time steps in the IMU time series can therefore be assigned a step length, depending on which two HS the corresponding time step lies between.

C. Gait Event Detector

For comparison, two distinct gait event detection algorithms were implemented: a rule-based peak detection approach and an ML-based approach using a convolutional sequence-to-sequence model (Seq2Seq), which are described in the following.

1) Rule-based: The HS detection strategy for this approach is motivated by the physical properties of the body. During gait, the body's center of gravity periodically undergoes vertical movements that allow HS detection by looking at the IMU's acceleration measurements in the vertical direction. Therefore, the identification of a HS event is possible by analyzing kinematic data, specifically focusing on the vertical velocity of the foot.

To detect HS events, the negative discrete integral of the measured acceleration from the IMU sensor in the vertical axis is computed. After integration, the Butterworth filter [34] with a cutoff frequency of $\omega = 0.08 \frac{\mathrm{rad}}{\mathrm{s}}$ and a filter order of $N = 4$ is

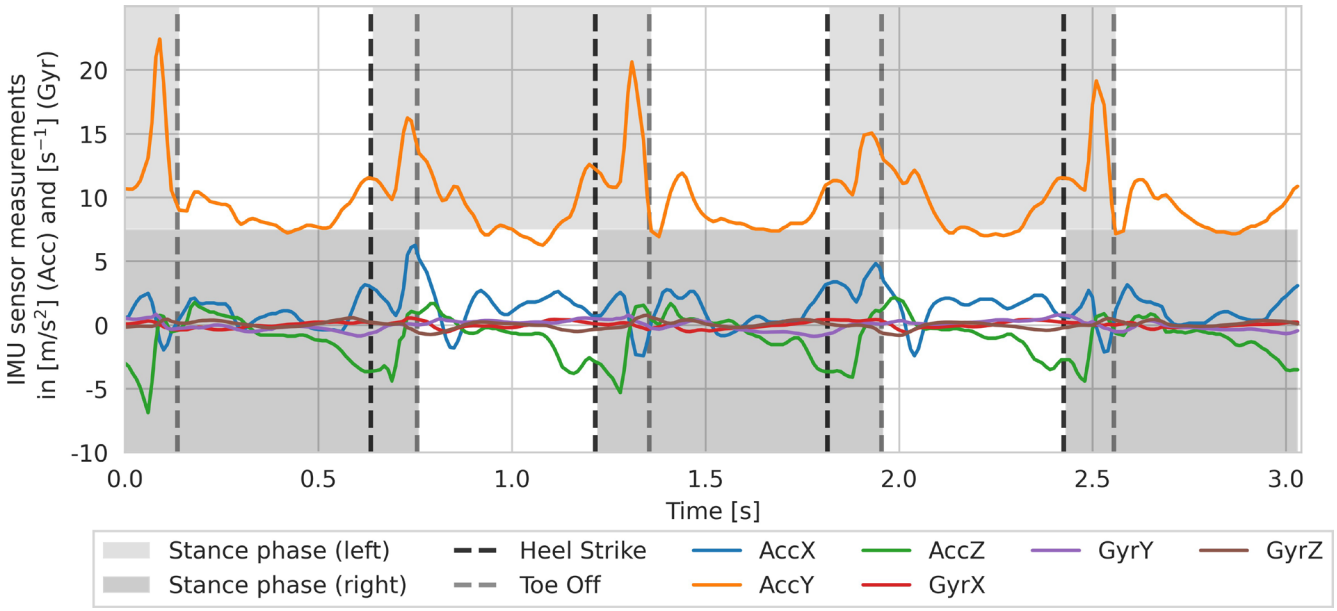

Fig. 3. Exemplary time series of measurements from the sensor belt (IMU-sensor) during a walk of a subject on a distance of 4 meters. The y-axis indicates the vertical direction, which is why the data of AccY shows an increased acceleration.

applied. This filters out high frequency oscillations, removing short-term influences on the signal in the form of noise and preserving the long-term signal curve. A peak detection with a minimum prominence of 0.1 m/s is performed subsequently. The peaks of this time series are then used as timestamps for HS estimations.

The TO events are detected correspondingly, except that the peaks are detected in the positive discrete integral of the vertical acceleration. A comparison of the results with those of the ML approach is given in Section IV-A.

Following the identification of the peak values for HS and TO, a linear regression is employed to minimize any systematic shifts. In order to identify the parameters of the linear regression, the data set is subjected to cross-evaluation. In this process, the complete data for one subject is withheld while the linear regression is conducted on the remaining data. The withheld data is then transformed according to the parameters identified in the previous step. This method is repeated for each subject.

2) ML-based: This section describes the approach for the ML-based step-event detection, using a convolutional Seq2Seq model. First, the main principles of the algorithm are introduced, followed by an explanation of the network architecture and the training phase.

The GAITRite® data contains the timings of the HS and TO events per walk, with the objective of estimating them. Each walk w_{ij} for subject i consists of HS timestamps $\mathbf{u}^{\mathrm{HS}}_{ij} = (u^{\mathrm{HS}}_1, u^{\mathrm{HS}}_2, \ldots, u^{\mathrm{HS}}_k)_{ij}$ and TO timestamps $\mathbf{u}^{\mathrm{TO}}_{ij} = (u^{\mathrm{TO}}_1, u^{\mathrm{TO}}_2, \ldots, u^{\mathrm{TO}}_l)_{ij}$. The number of gait events varies with each walk.

To make this data available to the neural network as input, each walk is encoded by a binary time series. Each HS marks a new step and is the start of the double support phase, meaning that two feet touching simultaneously the ground. In contrast to that, the single support phase is the phase where one foot touches the ground while the other is in the swing phase. Following, the binary gait-support representation encodes for each time step whether it is a single (0) or double support phase (1). In this representation, gait events are identifiable at the transition points from 0 to 1 or vice versa, as depicted in Fig. 4.

The network processes a time series window with a fixed length of 200 with a step-width of 1 sample and the six IMU-channels (acceleration and gyroscope measurements along the three spatial axes) as input, as visualized in Fig. 5). It produces an output time series of the same length with one channel.

Among the overlapping windows, the median of all binary gait-support estimations (potentially rounded) are calculated as final output estimation. Therefore, for each input time series $\mathbf{X}_{w_{ij}} \in \mathbf{R}^{N_{wij} \times 6}$ with sequence length $N_{w_{ij}} \geq 200$, the network $\mathsf{N}_{\mathrm{detector}}$ produces an output time series $\mathsf{N}_{\mathrm{detector}}(\mathbf{X}_{w_{ij}}) = (\hat{y}_1, y_2, \ldots, \hat{y}_{N_{wij}})$, where $\hat{y}_t \in \{0, 1\}$, representing the type of gait-support phase. The transitions in that time series are used to identify the HS and TO events:

$$\hat{y}_t = 0 \rightarrow \hat{y}_{t+1} = 1 \text{ indicates a HS event at time } t+1,$$
$$\hat{y}_t = 1 \rightarrow \hat{y}_{t+1} = 0 \text{ indicates a TO event at time } t+1,$$

resulting into two output vectors $(\hat{u}^{\mathrm{HS}}_1, \hat{u}^{\mathrm{HS}}_2, \ldots, \hat{u}^{\mathrm{HS}}_k)$ and $(\hat{u}^{\mathrm{TO}}_1, \hat{u}^{\mathrm{TO}}_2, \ldots, \hat{u}^{\mathrm{TO}}_k)$, where each value represents the estimated timestamp of either a HS or a TO of walk w_{ij}.

As visualized in Fig. 6, the neural network architecture consists of a three-layer 1D-CNN as encoder followed by a symmetrical set of deconvolutional layers. The encoded representation is concatenated with additional encoded meta-data inputs, obtained through a linear feed-forward network that encodes subject-specific meta-information (age, weight, leg-length for both feet, gender and height). Each feature in

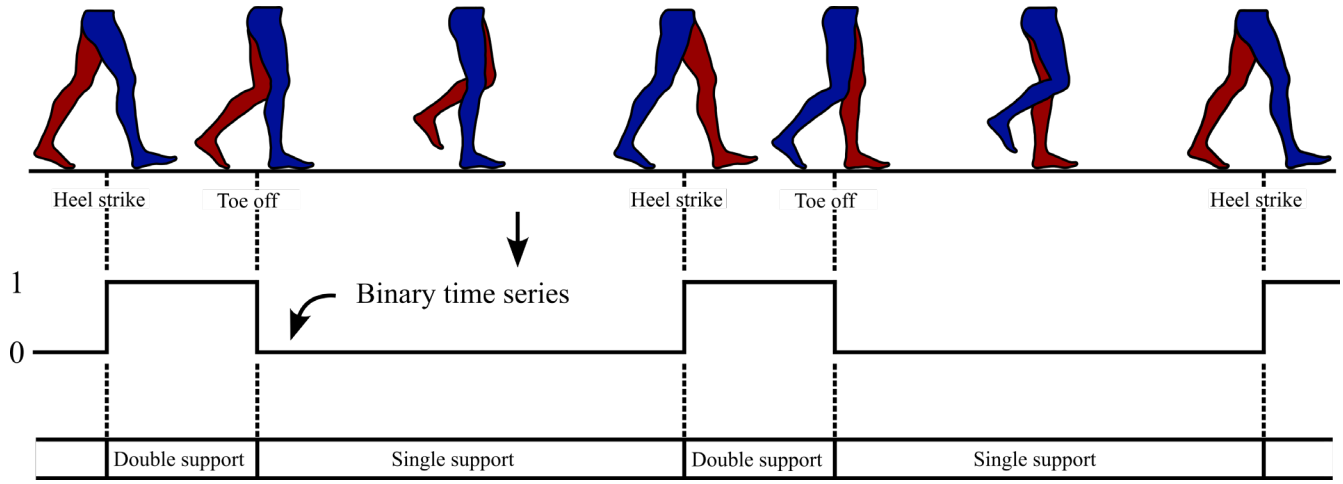

Fig. 4. Representation of the human gait cycle through a binary time series. A value of 1 means that the step is in the double support phase at the current time, while a value of 0 indicates single support. This representation is used as a trainable label. The transition between the two phases mark HS or TO events.

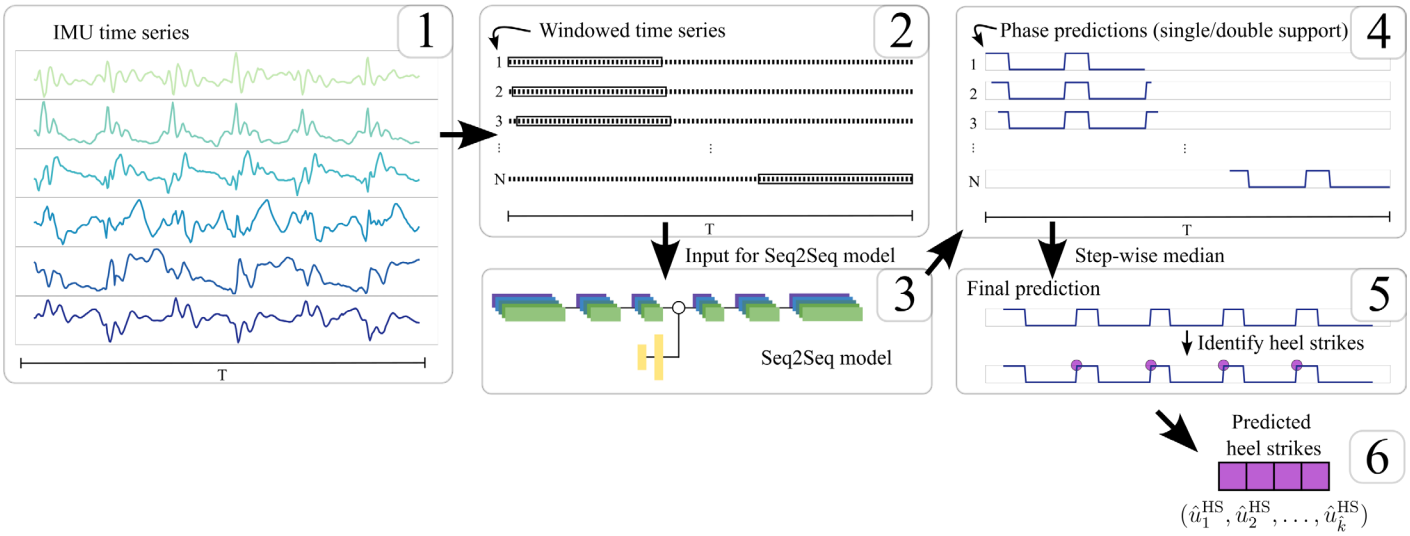

Fig. 5. Overview of our windowing approach to sample the time series (1) to same-length inputs (2) for the convolutional neural network (3). To create a final estimation, based on the original length of the time series, the median is calculated over the time axis to create a final estimation (4-6). Note, that the median of the values is only determined for the respective temporal overlapping estimations.

the meta-information is z-score normalized. In the evaluation, two versions were compared: one in which the encoded representation was used and one in which it was not.

The first two convolutional layers consist of 64 kernels with ReLU activation, batch normalization, and dropout. The third convolutional layer employs 32 kernels with a ReLU activation. The convolutional layers use a stride of 2 and maintain a fixed padding of 1 with a kernel size of 3. Subsequent deconvolutional layers mirror the same structure, leading to a single, sigmoid activated layer.

During training, time series of length 200 are sampled from the IMU data. A random offset is applied to each sample, and a sub-sequence of length 200 is then cut out. The AdamW optimizer [35] with a learning rate of 0.002, a weight decay of 0.01, and a batch size of 128 is used. The learning rate decreases by a factor of 2 as soon as the loss does not decrease over a span of six epochs. As loss function, the Binary-Cross-

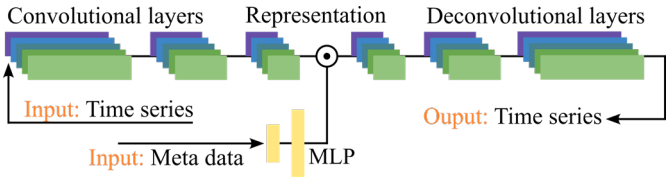

Fig. 6. Sequence-to-sequence model using 1-dimensional convolutional and deconvolutional kernels. Two versions of the model were trained and evaluated. One version concatenates additional encoded subject meta-information using a multi layer perceptron (MLP), while the other does not.

Entropy loss for the gait event estimation is used. The leave-one-out-cross evaluation (loo) is used to maximize the size of the training dataset. With loo, the complete data of a single subject is withheld at a time and the training is executed with the rest. Only the unseen data of the left out subject will be

evaluated. The evaluation results are averaged over all folds. The training is stopped early if the loss does not decrease over a span of 24 epochs, or if the maximum number of 72 epochs has been completed.

D. Step Length Regressor

In the following, the algorithm for step length estimation for each consecutive HS event is described. The estimation of step lengths is based on the same neural network architecture as the ML-based gait event detector (described in Sec. III-C.2). Only the last activation function (sigmoid), is replaced by the identity function.

The GAITRite® data contains a step length annotation for each consecutive HS. As a preparatory step, the step lengths of each walk w_{ij} are converted into a time series with the same length as the corresponding IMU data $\mathbf{X}_{w_{ij}}$ of that walk: For each time step within the time span in between two consecutive HS, the same step length is assigned, given by the GAITRite® data. The resulting time series $\mathbf{l}_{w_{ij}} = (l_1, l_2, \ldots, l_{N_{w_{ij}}})$, with $N_{w_{ij}}$ as total number of time steps within $\mathbf{X}_{w_{ij}}$ therefore looks like a step function (as visualized in Fig. 7). $\mathbf{l}_{w_{ij}}$ is to be estimated by the neural network, using the IMU data of a walk $\mathbf{X}_{w_{ij}}$ as $\mathsf{N}_{\text{regressor}}(\mathbf{X}_{w_{ij}}) =: \hat{\mathbf{l}}_{w_{ij}} \rightarrow \mathbf{l}_{w_{ij}}$.

Next, the HS event estimations from either the rule-based or ML-based approaches are used for calculating final step length estimations for each consecutive HS $(\hat{u}_i^{\text{HS}}, \hat{u}_{i+1}^{\text{HS}})_{w_i}$, with $i \in \{1, 2 \ldots, k-1\}$, where k is the number of estimated HS. The median of all estimations of the network $\mathsf{N}_{\text{regressor}}$ within the time spans between each consecutive HS is calculated. Additionally, a step length is estimated for the time span from time step 0 to the first estimated HS, resulting in a final estimation of step lengths $\hat{\mathbf{s}}_{w_{ij}} = (\hat{s}_1, \hat{s}_2, \ldots, \hat{s}_{\hat{k}})$. Note, that $\hat{k}$, the number of predicted step lengths may differ from the total number of step lengths, annotated by the GAITRite®.

For training, the same randomized sampling strategy as for the ML-based gait event detection is applied. Furthermore, loo-evaluation, optimizer, learning rate, weight decay, batch size, learning rate scheduler and early stopping strategy remain the same. The loss function used is the mean squared error.

E. Additional Gait Parameter Estimation

The following gait parameters are calculated by using the HS (from either the rule-based or ML-based algorithm) and the respective step lengths estimations from the ML-based algorithm:

Cadence: First, the inverse of the time between two consecutive HS is calculated, and the average is taken of all such values on each walk.

Velocity: The velocity is computed by dividing each estimated step length by its corresponding step time.

Step time: The step time is computed by subtracting the time of each estimated HS from the time of the previous HS.

Stance time: The stance time is computed by subtracting the time of each TO from the time of the previous HS.

Swing time: The swing time is computed by subtracting the time of each HS from the time of the previous TO.

These gait parameters are all evaluated walk-wise.

F. Evaluation

1) Gait Event Detector: For evaluation of gait event detection, each walk w_{ij} is divided into several segments. The segments are defined by the midpoint between consecutive gait events (either HS or TO) as the start and the midpoint between the next pair of gait events as the end using the annotations of HS and TO timestamps of the GAITRite® ($\mathbf{t}_{ij}^{\text{HS}}$, $\mathbf{t}^{\text{TO}}$). The time stamp of the left boundary of the first segment is set to 0, and the time stamp of the right boundary of the last segment is set to $N_{w_{ij}}$. This segmentation allows for the identification of each step in the series u_{ij} belonging to a single segment. A gait event (P_n^{HS} or P_n^{TO}) is correctly identified if it is the only one to occur in a segment. Segments with multiple estimations are marked as instances of over-estimation such that this segment is marked as false positive. Those without any estimations are regarded as false negatives. Using this segmentation approach, metrics such as accuracy, precision, recall, and the F1-score can be calculated as follows:

$$\text{Accuracy} = \frac{\text{TP}}{\text{N}},$$

$$\text{Precision} = \frac{\text{TP}}{\text{TP} + \text{FP}},$$

$$\text{Recall} = \frac{\text{TP}}{\text{TP} + \text{FN}},$$

$$\text{F1-score} = 2 \cdot \frac{\text{Precision} \cdot \text{Recall}}{\text{Precision} + \text{Recall}}.$$

However, true negatives are not calculated here, and therefore, the specificity is not calculated. N denotes the total number of steps. Note, that there is no true negative estimation, since we define the segments in a way, that they always contain exactly one gait event, and a definition of TN cannot be meaningfully defined here. The mean time difference between the estimated events and the GAITRite® reference measures ($\mathbf{t}_{ij}^{\text{HS}}$, $\mathbf{t}_{ij}^{\text{TO}}$) is calculated only for the TP segments.

2) Step Length Regressor: In the GAITRite® reference data, each walk w_{ij} has a varying amount of annotated step lengths $\mathbf{s}_{w_{ij}}$, which corresponds to the number of steps taken during the walk, which are defined by the number of HS occurring within w_{ij}. As a basis for evaluating step lengths, the steps must also be detected by the algorithm. When a HS $u_n^{\text{HS}} \in {}_i^{\text{HS}}$ is correctly detected (fulfilling the definition of a true positive according to III-F.1), the corresponding step length estimation $\hat{s}_n \in \hat{\mathbf{s}}_{w_{ij}}$ is used to calculate the error with $s_n \in \mathbf{s}_{w_{ij}}$. The error measure is the absolute error.

IV. Results

The gait event detection is evaluated for all three approaches, the rule-based and the ML-based (with and without subject related meta-information). Afterward, the accuracy of the step length regressor and the resulting additional gait parameters (cadence, velocity, step time, stance time and swing time) are evaluated.

A. Evaluation of Gait Event Detection

The evaluation of the gait event detectors (rule-based and ML-based) are presented in Table III and IV. The ML-based

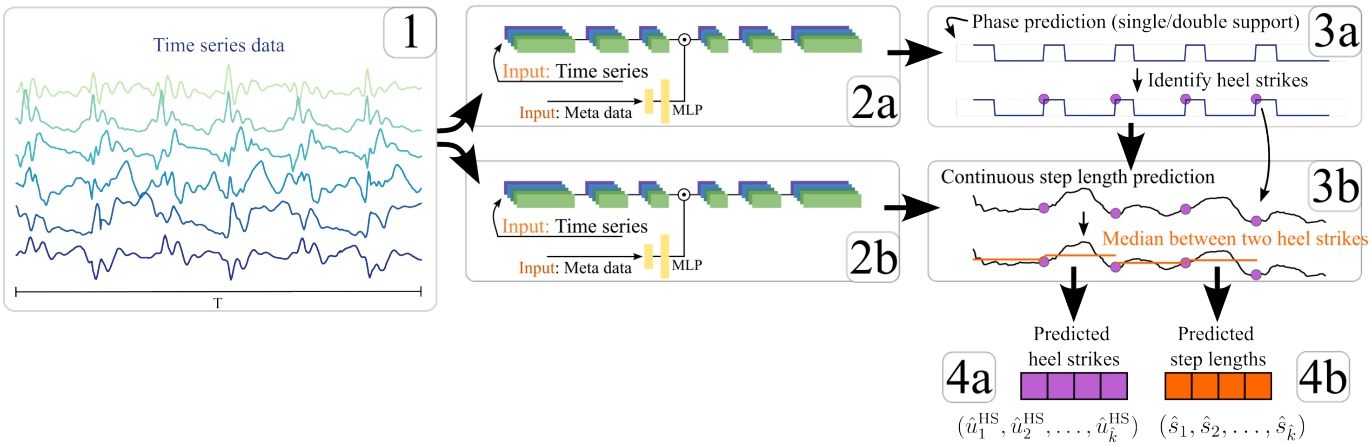

Fig. 7. Combined HS detection and step length regression using a convolution neural network as a Seq2Seq model with a windowing approach. The time series data from the sensor belt are fed as input (1) to the neural network (2a) which provides an estimation whether each time step is within a double or single support phase (3a). Based on this, the HS are identified as phase change from the single support to the double support phase (4a). The neural network for step length estimation uses the same input data (2b) and estimates for each time step a step length. The timestamps of the HS estimations are then used to average the section between neighboring events of the step length estimations (3b). Such averages are then used as the final step length estimation (4b).

approach is evaluated with and without the inclusion of meta-information. The accuracy, precision, recall and F1 score are for all three evaluated approaches over 99% or slightly below (see Table III). The ML-based approach with meta-information shows the best performance in temporally closely predicting the HS and TO events, following by the ML-based without meta-information. The rule-based approach performs worst (Table IV).

TABLE III
ACCURACY, PRECISION, RECALL AND F1-SCORE OF THE HEEL STRIKE (HS) AND TOE OFF (TO) DETECTIONS.

Metric	Method	HS	TO
Accuracy	Rule-based	99.24%	98.45%
	ML-based (without meta-info)	98.89%	99.20%
	ML-based (with meta-info)	99.19%	99.30%
Precision	Rule-based	99.38%	99.81%
	ML-based (without meta-info)	98.89%	99.46%
	ML-based (with meta-info)	99.19%	99.56%
Recall	Rule-based	99.86	99.64%
	ML-based (without meta-info)	99.99 %	99.74%
	ML-based (with meta-info)	99.99 %	99.74%
F1 score	Rule-based	99.62%	99.72%
	ML-based (without meta-info)	99.44%	99.60%
	ML-based (with meta-info)	99.59%	99.65%

TABLE IV
TEMPORAL DEVIATION BETWEEN ESTIMATED GAIT EVENTS TIMINGS AND THE TRUE EVENT TIMINGS, WHICH IS QUANTIFIED BY THE MEAN ABSOLUTE ERROR (MAE) AND MEAN ERROR (ME) WITH STANDARD DEVIATION (SD).

Metric	Method	MAE	ME±SD
HS [ms]	Rule-based	28.9	-3.10±39.4
	ML-based (without meta-info)	21.41	-2.45±34.23
	ML-based (with meta-info)	21.84	-2.81±34.14
TO [ms]	Rule-based	44.33	0.33±57.72
	ML-based(without meta-info)	23.71	-3.50±38.75
	ML-based(with meta-info)	23.19	-3.77±38.09

B. Evaluation of Step Length Regression and Additional Gait Parameters

The evaluation of the step length regressor algorithm and the derived additional gait parameters are summarized in Table V. For all gait parameters, the ML-based approach with meta-information performs best, followed by the ML-based approach without meta-information. The rule-based approach shows the poorest performance for all gait parameters. Only for the parameters cadence and velocity does rule-based perform better than ML-based without meta-information.

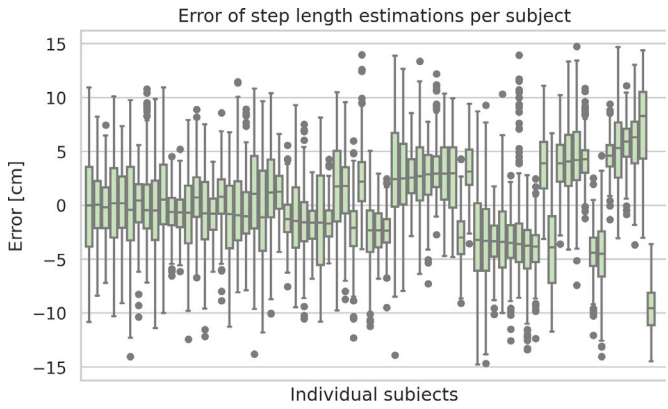

Fig. 8. Box plots of the estimation errors of the step lengths for each subject.

Consequently, the algorithmic combination of ML-based event detection and ML-based step length estimation with the inclusion of meta-information is considered for further evaluation, as it demonstrated the best performance overall compared to the combination of a rule-based event detection with the ML-based step length regression.

Figure 8 displays box plots of the per-subject step length error, which differ depending on the subject. The error for some subjects exhibits a systematic bias, whereas for others it is nearly absent. The same kind of plot for the remaining

TABLE V
GAIT PARAMETER ESTIMATION ERRORS WITH MEAN ERROR (ME)Y STANDARD DEVIATION (SD), AND THE PEARSON CORRELATION COEFFICIENT (CC)

Gait parameter	HS detection method	ME±SD	CC
Step length [cm]	Rule-based	0.61 ± 5.29	0.81
	ML-based (without meta-info)	0.62 ± 5.20	0.81
	ML-based (with meta-info)	-0.12 ± 4.49	0.83
Cadence [$\frac{1}{min}$]	Rule-based	0.8401 ± 6.193	0.86
	ML-based (without meta-info)	0.2239 ± 7.1957	0.81
	ML-based (with meta-info)	0.1305 ± 6.9086	0.83
Velocity [$\frac{m}{s}$]	Rule-based	-0.0025 ± 0.0701	0.82
	ML-based (without meta-info)	-0.0020 ± 0.0704	0.81
	ML-based (with meta-info)	-0.0005 ± 0.0618	0.89
Step time [ms]	Rule-based	-3.978 ± 47.832	0.75
	ML-based (without meta-info)	-1.182 ± 40.810	0.80
	ML-based (with meta-info)	-0.036 ± 30.965	0.87
Stance time [ms]	Rule-based	8.50 ± 60.08	0.08
	ML-based (without meta-info)	-2.53 ± 31.76	0.54
	ML-based (with meta-info)	-2.13 ± 31.54	0.54
Swing time [ms]	Rule-based	-5.21 ± 65.09	0.38
	ML-based (without meta-info)	-0.11 ± 46.96	0.57
	ML-based (with meta-info)	1.42 ± 38.63	0.66

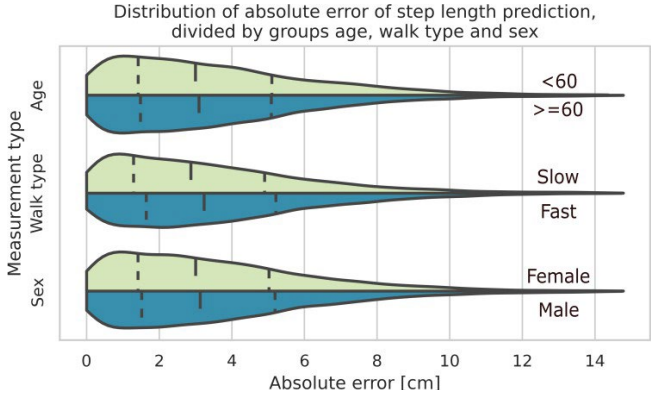

Fig. 9. Distribution of absolute errors of estimated step lengths, segmented according to age groups, types of walk, and gender. The biggest error difference is in the walk type, where the error is higher for fast gaits. However, the average step length is also bigger for these walks. Subsequently, the percentage error between the walk types does not differ much (4.81% for slow walks compared to 4.94% for fast walks).

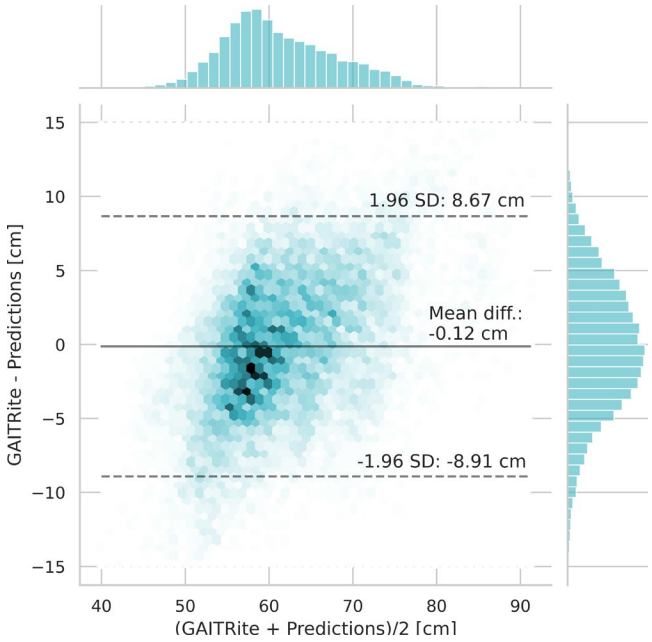

Fig. 10. Bland Altman plot of the step lengths estimations and reference values.

considered gait parameters is shown in the appendix. The absolute error of step length regression for subjects under 60 years old, compared to those 60 years old and above, is not significant (p-value< 0.05) according to the Mann-Whitney U test. However, when the data is grouped by walk type (slow and fast) and gender, a significant difference is observed (p-value< 0.05). Figure 9 presents a violin plot [36] that shows the kernel density estimations for each individual group in direct comparison with their counterparts. The dotted lines represent the median value and the quartiles, respectively. Fig. 10 shows the Bland Altman [37] plot for the step length estimation of the ML-based algorithm. The mean difference is -0.12 cm with a 1.96 SD interval of [-8.91 cm, 8.67 cm].

V. DISCUSSION

A rule-based approach and a data-driven ML-based approach for detecting the HS and TO events and for estimating six gait parameters via time series-data of an IMU sensor belt was presented. The performance of both approaches for estimating the gait events has been evaluated regarding the accuracy, precision, recall and F1 score. Based on the HS events, the step length is estimated via a step length regressor. Subsequently, based on the detected HS events and estimated step lengths, the additional gait parameters velocity, cadence, step time, stance time, and swing time were calculated.

The study compared rule-based and ML methods for detecting gait events and found that the ML-based (ML-Seq2Seq) method was more precise in predicting the timing of these events. Specifically, the rule-based method's predictions of the timings for HS events were on average more displaced, com-

TABLE VI
COMPARISON OF RESULTS FROM PREVIOUS STUDIES WITH OUR ML-BASED APPROACH - TEMPORAL GAIT PARAMETERS.

Sensor placement	Author	Stride time [s]	Step time [s]	Stance time [s]	Swing time [s]	Cadence [1/min]
Shank	[22]	0.006±0.002	0.009±0.004	0.044±0.013	N/A	N/A
	[31]	0.0±0.03	N/A	-0.01±0.04	0.0±0.03	0.6±5.4
	[33]	-0.021±0.091	-0.008±0.041	N/A	N/A	0.589±1.144
Feet	[32]	0±0.07	N/A	0±0.07	0±0.05	N/A
	[31]	-0.01±0.04	N/A	-0.01±0.03	-0.01±0.03	1.2± 6.0
Waist	[22]	0.006±0.001	0.009±0.003	0.013±0.012	N/A	N/A
	ML-based (with meta-info)	N/A	0.0±0.031	-0.002±0.032	0.001±0.039	0.13± 6.91

TABLE VII
COMPARISON OF RESULTS FROM PREVIOUS STUDIES WITH OUR ML-BASED APPROACH (ML-SEQ2SEQ) - SPATIAL GAIT PARAMETERS.

Sensor placement	Author	Stride length [cm]	Step length [cm]	Step width [cm]
Shank	Storm [22]	N/A	N/A	N/A
	Renani [31]	0.4±9.7	-0.6±5.6	0.85±4.6
	Skvortsov [33]	N/A	N/A	N/A
Feet	Hannink [32]	-0.15±6.09	N/A	-0.09±4.22
	Renani [31]	-3.0±8.7	-1.7±5.2	1.1±5.1
Waist	Storm [22]	N/A	N/A	N/A
	ML-based (with meta-info)	N/A	-0.12±4.49	N/A

pared to the ML-based method. The results indicate that there was a slight improvement in HS and TO detection from the ML-based approach without meta-information to the approach which uses meta-information. Incorporating meta-information in the ML-based method also led to an improvement in gait parameter estimation.

The step length regression, using the estimated HS events, shows comparable performance for both the ML-based and rule-based approaches. This observation also extends to the derived gait parameters of cadence and velocity.

It is challenging to make direct comparisons between our results and related work due to the influence of various factors, including differences in dataset size, reference systems, the route of the course (e.g., straight ahead, on a staircase, or going around a bend), evaluation metrics, or subject cohorts (e.g., healthy or diseased, or demographic characteristics). However, we do compare individual gait parameters by focusing on publications that implement gait analysis on healthy subjects on a straight course. Tables VI and VII show the results of previous studies in comparison with the results of our ML-based approach (with the use of meta-information).

The ML-based approach employs a windowing approach and requires a minimum time series length of two seconds in this instance. Consequently, the algorithm can be used in a streaming approach, whereby the results may be updated with each new time step in real time. In the initial phase, a minimum of two seconds of historical data is required. The proposed algorithm is designed to accommodate an arbitrary number of sensor channels. It is also possible to combine several sensors (in our case, we used one sensor, which resulted in six channels for the acceleration and angular velocity). To date, the algorithm has been developed for the purpose of detecting gait parameters during walking. During running and sprinting, the body is not in contact with the ground for a certain period of time, which makes it impossible to detect gait events using the binary representation of the gait cycle, which represents single and double support phases. Nevertheless, an extension of the algorithm is planned to be developed in order to detect gait events during these gaits. This extension will consider not only double and single support phases, but also a phase of *no support*. Furthermore, the algorithm is constrained to the identification of HS and TO. Other gait events, such as heel off and toe on, are not detectable through this approach. We anticipate validating the ML-based approach with additional datasets to confirm the clinical meaningfulness of the derived gait parameters in additional cohorts and disease groups.

APPENDIX

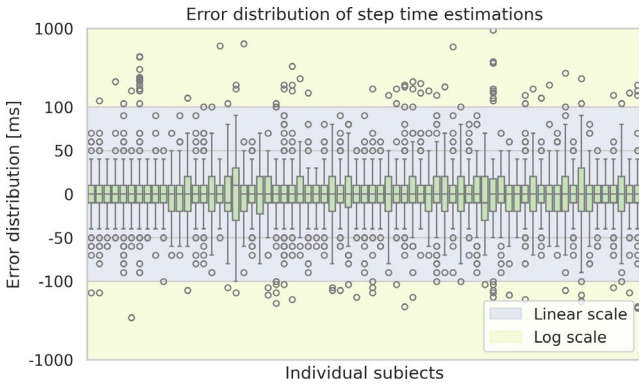

Fig. 11. Box plots of the estimation errors of the step time estimations for each subject.

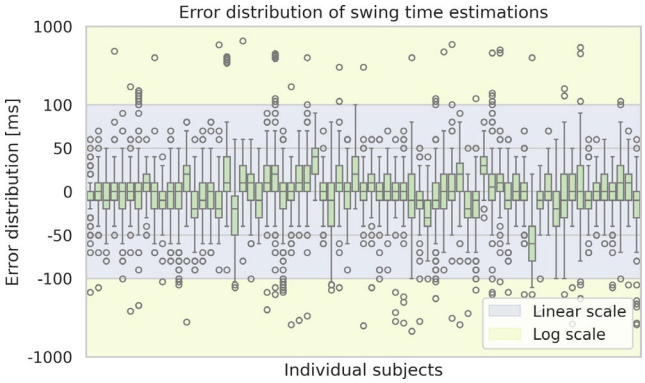

Fig. 12. Box plots of the estimation errors of the swing time estimations for each subject.

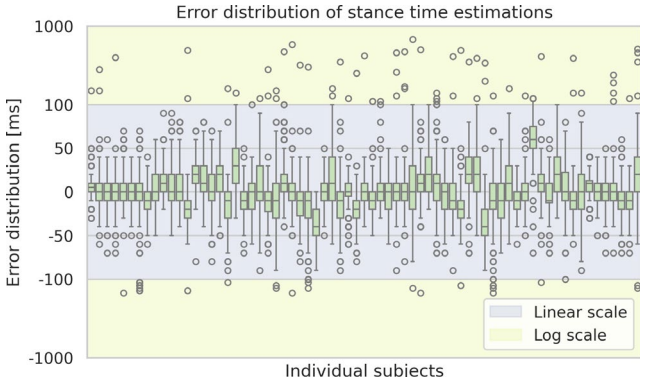

Fig. 13. Box plots of the estimation errors of the stance time estimations for each subject.

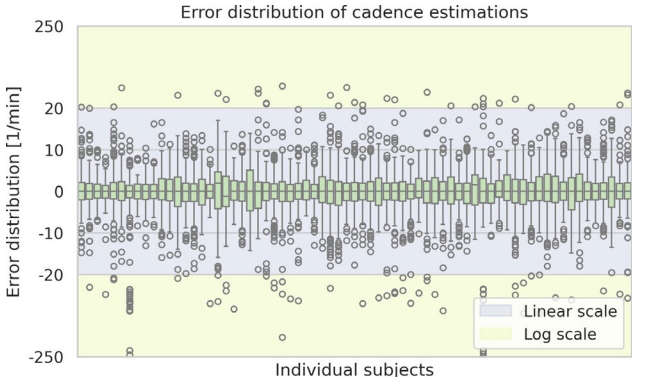

Fig. 14. Box plots of the estimation errors of the cadence estimations for each subject.

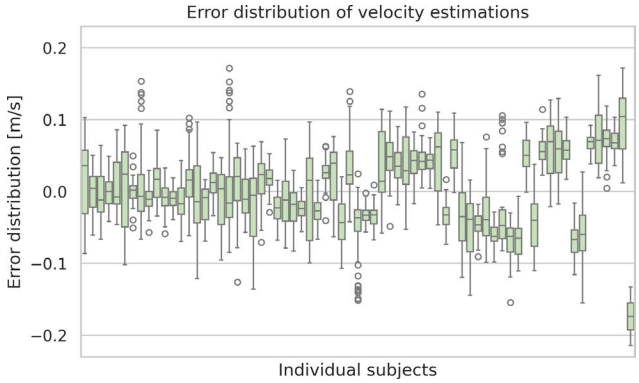

Fig. 15. Box plots of the estimation errors of the velocity estimations for each subject.

ACKNOWLEDGMENTS

The author thank all participants of the study for their time and effort. We acknowledge financial support by the German Federal Ministry of Education and Research (01ZZ2007).

REFERENCES

[1] J. Verghese, R. Holtzer, R. B. Lipton, and C. Wang, "Quantitative Gait Markers and Incident Fall Risk in Older Adults," *The Journals of Gerontology Series A: Biological Sciences and Medical Sciences*, vol. 64A, no. 8, p. 896–901, Apr. 2009. [Online]. Available: https://academic.oup.com/biomedgerontology/article/64A/8/896/664600

[2] S. Fudickar, J. Kiselev, C. Stolle, T. Frenken, E. Steinhagen-Thiessen, S. Wegel, and A. Hein, "Validation of a Laser Ranged Scanner-Based Detection of Spatio-Temporal Gait Parameters Using the aTUG Chair," *Sensors*, vol. 21, no. 4, p. 1343, Feb. 2021. [Online]. Available: https://www.mdpi.com/1424-8220/21/4/1343

[3] A. Weiss, M. Brozgol, M. Dorfman, T. Herman, S. Shema, N. Giladi, and J. M. Hausdorff, "Does the Evaluation of Gait Quality During Daily Life Provide Insight Into Fall Risk? A Novel Approach Using 3-Day Accelerometer Recordings," *Neurorehabilitation and Neural Repair*, vol. 27, no. 8, p. 742–752, Jun. 2013. [Online]. Available: https://journals.sagepub.com/doi/10.1177/1545968313491004

[4] M. Pistacchi, M. Gioulis, F. Sanson, E. D. Giovannini, G. Filippi, F. Rossetto, and S. Z. Marsala, "Gait analysis and clinical correlations in early Parkinsons disease," *Functional Neurology*, vol. 32, no. 1, pp. 28–34, Jan 2017. [Online]. Available: https://www.ncbi.nlm.nih.gov/pmc/articles/PMC5505527/

[5] J. Wilson, L. Alcock, A. J. Yarnall, S. Lord, R. A. Lawson, R. Morris, J.-P. Taylor, D. J. Burn, L. Rochester, and B. Galna, "Gait Progression Over 6 Years in Parkinson's Disease: Effects of Age, Medication, and Pathology," *Frontiers in Aging Neuroscience*, vol. 12, Oct. 2020. [Online]. Available: https://www.frontiersin.org/articles/10.3389/fnagi.2020.577435/full

[6] S. Studenski, "Gait Speed and Survival in Older Adults," *JAMA*, vol. 305, no. 1, p. 50, Jan 2011. [Online]. Available: https://jamanetwork.com/journals/jama/fullarticle/644554

[7] S.-Y. Chien, M.-C. Chuang, and I.-P. Chen, "Why People Do Not Attend Health Screenings: Factors That Influence Willingness to Participate in Health Screenings for Chronic Diseases," *International Journal of Environmental Research and Public Health*, vol. 17, no. 10, p. 3495, May 2020. [Online]. Available: https://www.mdpi.com/1660-4601/17/10/3495

[8] S. Vítecˇková, H. Horáková, K. Poláková, R. Krupicˇka, E. Ruˇžicˇka, and H. Brožová, "Agreement between the GAITRite® System and the Wearable Sensor BTS G-Walk® for measurement of gait parameters in healthy adults and Parkinson's disease patients," *PeerJ*, vol. 8, p. e8835, May 2020. [Online]. Available: https://peerj.com/articles/8835/

[9] K. E. Webster, J. E. Wittwer, and J. A. Feller, "Validity of the GAITRite® walkway system for the measurement of averaged and individual step parameters of gait," *Gait & Posture*, vol. 22, no. 4, p. 317–321, Dec. 2005. [Online]. Available: https://www.sciencedirect.com/science/article/abs/pii/S0966636204002061?via%3Dihub

[10] A. Steinert, I. Sattler, K. Otte, H. Röhling, S. Mansow-Model, and U. Müller-Werdan, "Using new camera-based technologies for gait analysis in older adults in comparison to the established gaitrite system," *Sensors*, vol. 20, no. 1, p. 125, Dec. 2019. [Online]. Available: https://www.mdpi.com/1424-8220/20/1/125

[11] L. C. Büker, F. Zuber, A. Hein, and S. Fudickar, "HRDepthNet: Depth Image-Based Marker-Less Tracking of Body Joints," *Sensors*, vol. 21, no. 4, p. 1356, Feb. 2021. [Online]. Available: https://www.mdpi.com/1424-8220/21/4/1356

[12] J. Stenum, C. Rossi, and R. T. Roemmich, "Two-dimensional

video-based analysis of human gait using pose estimation," *PLOS Computational Biology*, vol. 17, no. 4, p. e1008935, Apr. 2021. [Online]. Available: https://journals.plos.org/ploscompbiol/article?id=10.1371/journal.pcbi.1008935

[13] M. Dunn, A. Kennerley, Z. Murrell-Smith, K. Webster, K. Middleton, and J. Wheat, "Application of video frame interpolation to markerless, single-camera gait analysis," *Sports Engineering*, vol. 26, no. 1, Apr. 2023. [Online]. Available: https://link.springer.com/article/10.1007/s12283-023-00419-3

[14] H. Prasanth, M. Caban, U. Keller, G. Courtine, A. Ijspeert, H. Vallery, and J. von Zitzewitz, "Wearable Sensor-Based Real-Time Gait Detection: A Systematic Review," *Sensors*, vol. 21, no. 8, p. 2727, Apr. 2021. [Online]. Available: https://www.mdpi.com/1424-8220/21/8/2727

[15] S. Hellmers, B. Izadpanah, L. Dasenbrock, R. Diekmann, J. Bauer, A. Hein, and S. Fudickar, "Towards an Automated Unsupervised Mobility Assessment for Older People Based on Inertial TUG Measurements," *Sensors*, vol. 18, no. 10, p. 3310, Oct. 2018. [Online]. Available: https://www.mdpi.com/1424-8220/18/10/3310

[16] M. Ullrich, N. Roth, A. Kuderle, R. Richer, T. Gladow, H. Gasner, F. Marxreiter, J. Klucken, B. M. Eskofier, and F. Kluge, "Fall Risk Prediction in Parkinson's Disease Using Real-World Inertial Sensor Gait Data," *IEEE Journal of Biomedical and Health Informatics*, vol. 27, no. 1, p. 319–328, Jan 2023. [Online]. Available: https://ieeexplore.ieee.org/document/9924545

[17] C. Kirk and e. a. Küderle, "Mobilise-D insights to estimate real-world walking speed in multiple conditions with a wearable device," *Scientific Reports*, vol. 14, no. 1, Jan 2024. [Online]. Available: https://www.nature.com/articles/s41598-024-51766-5

[18] A. L. McDonough, M. Batavia, F. C. Chen, S. Kwon, and J. Ziai, "The validity and reliability of the GAITRite system's measurements: A preliminary evaluation," *Archives of Physical Medicine and Rehabilitation*, vol. 82, no. 3, p. 419–425, Mar. 2001. [Online]. Available: https://www.archives-pmr.org/article/S0003-9993(01)23717-4/abstract

[19] R. J. Mobbs, J. Perring, S. M. Raj, M. Maharaj, N. K. M. Yoong, L. W. Sy, R. D. Fonseka, P. Natarajan, and W. J. Choy, "Gait metrics analysis utilizing single-point inertial measurement units: a systematic review," *mHealth*, vol. 8, p. 9–9, Jan. 2022. [Online]. Available: https://mhealth.amegroups.org/article/view/80258/html

[20] A. Keogh, R. Argent, A. Anderson, B. Caulfield, and W. Johnston, "Assessing the usability of wearable devices to measure gait and physical activity in chronic conditions: a systematic review," *Journal of NeuroEngineering and Rehabilitation*, vol. 18, no. 1, Sep 2021. [Online]. Available: https://jneuroengrehab.biomedcentral.com/articles/10.1186/s12984-021-00931-2

[21] G. Cicirelli, D. Impedovo, V. Dentamaro, R. Marani, G. Pirlo, and T. R. D'Orazio, "Human Gait Analysis in Neurodegenerative Diseases: A Review," *IEEE Journal of Biomedical and Health Informatics*, vol. 26, no. 1, p. 229–242, Jan. 2022. [Online]. Available: https://ieeexplore.ieee.org/document/9466394

[22] F. A. Storm, C. J. Buckley, and C. Mazzà, "Gait event detection in laboratory and real life settings: Accuracy of ankle and waist sensor based methods," *Gait & Posture*, vol. 50, p. 42–46, Oct. 2016. [Online]. Available: https://www.sciencedirect.com/science/article/pii/S096663621630488X?via%3Dihub

[23] S. Bertuletti, U. Della Croce, and A. Cereatti, "A wearable solution for accurate step detection based on the direct measurement of the inter-foot distance," *Journal of Biomechanics*, vol. 84, p. 274–277, Feb. 2019. [Online]. Available: https://www.sciencedirect.com/science/article/abs/pii/S0021929018309382?via%3Dihub

[24] R. Romijnders, E. Warmerdam, C. Hansen, J. Welzel, G. Schmidt, and W. Maetzler, "Validation of IMU-based gait event detection during curved walking and turning in older adults and Parkinson's Disease patients," *Journal of NeuroEngineering and Rehabilitation*, vol. 18, no. 1, Feb. 2021. [Online]. Available: https://jneuroengrehab.biomedcentral.com/articles/10.1186/s12984-021-00828-0

[25] G. Pacini Panebianco, M. C. Bisi, R. Stagni, and S. Fantozzi, "Analysis of the performance of 17 algorithms from a systematic review: Influence of sensor position, analysed variable and computational approach in gait timing estimation from IMU measurements," *Gait & Posture*, vol. 66, p. 76–82, Oct. 2018. [Online]. Available: https://www.sciencedirect.com/science/article/abs/pii/S0966636218304004?via%3Dihub

[26] R. Romijnders, E. Warmerdam, C. Hansen, G. Schmidt, and W. Maetzler, "A Deep Learning Approach for Gait Event Detection from a Single Shank-Worn IMU: Validation in Healthy and Neurological Cohorts," *Sensors*, vol. 22, no. 10, p. 3859, May 2022. [Online]. Available: https://www.mdpi.com/1424-8220/22/10/3859

[27] O. Dehzangi, M. Taherisadr, and R. ChangalVala, "IMU-Based Gait Recognition Using Convolutional Neural Networks and Multi-Sensor Fusion," *Sensors*, vol. 17, no. 12, p. 2735, Nov. 2017. [Online]. Available: https://www.mdpi.com/1424-8220/17/12/2735

[28] R. Moura Coelho, J. Gouveia, M. A. Botto, H. I. Krebs, and J. Martins, "Real-time walking gait terrain classification from foot-mounted Inertial Measurement Unit using Convolutional Long Short-Term Memory neural network," *Expert Systems with Applications*, vol. 203, p. 117306, Oct. 2022. [Online]. Available: https://www.sciencedirect.com/science/article/pii/S0957417422006698?via%3Dihub

[29] M. Z. Arshad, A. Jamsrandorj, J. Kim, and K.-R. Mun, "Gait Events Prediction Using Hybrid CNN-RNN-Based Deep Learning Models through a Single Waist-Worn Wearable Sensor," *Sensors*, vol. 22, no. 21, p. 8226, Oct. 2022. [Online]. Available: https://www.mdpi.com/1424-8220/22/21/8226

[30] M. Zago, M. Tarabini, M. Delfino Spiga, C. Ferrario, F. Bertozzi, C. Sforza, and M. Galli, "Machine-Learning Based Determination of Gait Events from Foot-Mounted Inertial Units," *Sensors*, vol. 21, no. 3, p. 839, Jan. 2021. [Online]. Available: https://www.mdpi.com/1424-8220/21/3/839

[31] M. Sharifi Renani, C. A. Myers, R. Zandie, M. H. Mahoor, B. S. Davidson, and C. W. Clary, "Deep Learning in Gait Parameter Prediction for OA and TKA Patients Wearing IMU Sensors," *Sensors*, vol. 20, no. 19, p. 5553, Sep. 2020. [Online]. Available: https://www.mdpi.com/1424-8220/20/19/5553

[32] J. Hannink, T. Kautz, C. F. Pasluosta, K.-G. Gasmann, J. Klucken, and B. M. Eskofier, "Sensor-Based Gait Parameter Extraction With Deep Convolutional Neural Networks," *IEEE Journal of Biomedical and Health Informatics*, vol. 21, no. 1, p. 85–93, Jan. 2017. [Online]. Available: https://ieeexplore.ieee.org/document/7778173

[33] D. Skvortsov, D. Chindilov, N. Painev, and A. Rozov, "Heel-Strike and Toe-Off Detection Algorithm Based on Deep Neural Networks Using Shank-Worn Inertial Sensors for Clinical Purpose," *Journal of Sensors*, vol. 2023, p. 1–9, May 2023. [Online]. Available: https://www.hindawi.com/journals/js/2023/7538611/

[34] S. Butterworth, "On the theory of filter amplifiers," *Experimental Wireless and the Wireless Engineer*, vol. 7, pp. 536–541, 1930.

[35] I. Loshchilov and F. Hutter, "Decoupled Weight Decay Regularization," Nov. 2017. [Online]. Available: https://arxiv.org/abs/1711.05101

[36] J. L. Hintze and R. D. Nelson, "Violin plots: A box plot-density trace synergism," *The American Statistician*, vol. 52, no. 2, p. 181–184, May 1998. [Online]. Available: https://www.jstor.org/stable/2685478?origin=JSTOR-pdf

[37] J. Martin Bland and D. Altman, "Statistical methods for assessing agreement between two methods of clinical measurement," *The Lancet*, vol. 327, no. 8476, p. 307–310, Feb. 1986. [Online]. Available: https://www.thelancet.com/journals/lancet/article/PIIS0140-6736(86)90837-8/fulltext

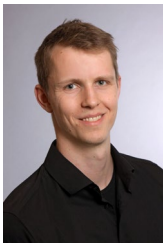

Roland Stenger (roland.stenger@uni-luebeck.de) is a Ph.D. student in the Institute for Medical Informatics, University of Lübeck, Germany. He received his M.Sc. in Physics from the University of Göttingen, Germany. His major research interests include the utilization of medical data and time series analysis, particularly for movement disorders.

Hawzhin Hozhabr Pour (hawzhin.hozhabrpour@uni-luebeck.de)
Hawzhin Hozhabr Pour is a postdoctoral researcher at the University of Lübeck's Institute of Medical Informatics. She completed her PhD at the University of Siegen, focusing on anomaly detection and event detection using artificial intelligence in time series data. Currently, she is a member of the junior research group MoveGroup, where her work centers on integrating and analyzing multi modal sensor signals and clinical data to enhance diagnostics and investigations of neurological movement disorders.

Jonas Teich (jonas.teich@web.de) is currently pursuing a master's degree in Data Science at the University of Hagen. He received a bachelor's degree in Business Informatics from the University of Oldenburg in 2023.

Andreas Hein (andreas.hein@uol.de) is full professor for Automation and Measurement Technologies at the Department for Health Services Research, Carl von Ossietzky University Oldenburg, Germany. He received his Diploma in Technical Computer Science and his PhD from the Technical University Berlin, Germany. His major research interests include: behavior and mobility analysis, analysis of vital data and biomechanical analysis and human-robot interaction.

Sebastian Fudickar (sebastian.fudickar@uni-luebeck.de) is the head of the MOVE Group junior research group at the University of Lübeck, Germany, which conducts research in the field of multimodal data analytics of wearable sensors as digital biomarkers. He holds a habilitation in medical informatics from the University of Lübeck and a PhD.